

MASS-TO-RADIUS RATIO FOR THE MILLISECOND PULSAR J0437–4715

G. G. PAVLOV

Pennsylvania State University, 525 Davey Lab, University Park, PA 16802; pavlov@astro.psu.edu

AND

V. E. ZAVLIN

Max-Planck-Institut für Extraterrestrische Physik, D-85740 Garching, Germany; zavlin@rosat.mpe-garching.mpg.de

Received 1997 June 24; accepted 1997 September 25; published 1997 October 23

ABSTRACT

Properties of X-ray radiation emitted from the polar caps of a radio pulsar depend not only on the cap temperature, size, and position, but also on the surface chemical composition, magnetic field, and neutron star's mass and radius. Fitting the spectra and the light curves with neutron star atmosphere models enables one to infer these parameters. As an example, we present here results obtained from the analysis of the pulsed X-ray radiation of a nearby millisecond pulsar, J0437–4715. In particular, we show that stringent constraints on the mass-to-radius ratio can be obtained if orientations of the magnetic and rotation axes are known, e.g., from the radio polarization data.

Subject headings: pulsars: individual (PSR J0437–4715) — stars: neutron — X-rays: stars

1. INTRODUCTION

Virtually all of the different models of radio pulsars (e.g., Cheng & Ruderman 1980; Arons 1981; Michel 1991; Beskin, Gurevich, & Istomin 1993) predict a common phenomenon: the presence of polar caps (PCs) around the neutron star (NS) magnetic poles heated up to X-ray temperatures by the backward accretion of relativistic particles and gamma-quanta from the pulsar magnetosphere. A typical size of the PC is estimated to be close to the radius within which the open magnetic field lines originate from the NS surface, $R_{pc} \sim (2\pi R^3/Pc)^{1/2}$ (~ 0.1 – 3 km for the period $P \sim 2$ s– 2 ms). However, expected PC temperatures, $T_{pc} \sim 5 \times 10^5$ – 5×10^6 K, and luminosities, $L_{pc} \sim 10^{28}$ – 10^{32} ergs s $^{-1}$, are much less certain and strongly depend on the specific pulsar model. Studying X-ray radiation from the PCs is particularly useful in discriminating between different models.

The best candidates for the investigation of the PC radiation are nearby, old pulsars with ages of $\tau \gtrsim 10^6$ yr, including very old millisecond pulsars, for which the NS surface outside the PCs is expected to be so cold, $T \lesssim 10^5$ K, that its thermal radiation is negligibly faint in the soft X-ray range. Indeed, available observational data allow one to assume the PC origin of soft X-rays detected from, e.g., PSR B1929+10 (Yancopoulos, Hamilton, & Helfand 1994; Wang & Halpern 1997), B0950+08 (Manning & Willmore 1994; Wang & Halpern 1997), and J0437–4715 (Becker & Trümper 1993). Moreover, there are some indications that hard tails of the X-ray spectra of younger pulsars, B0656+14 and B1055–52, may contain a thermal PC component (Greiveldinger et al. 1996). On the other hand, nonthermal (e.g., magnetospheric) X-ray radiation may dominate even in very old pulsars (cf. Becker & Trümper 1997). For example, ASCA observations of the millisecond pulsar B1821–24 (Saito et al. 1997), whose luminosity in the 0.5–10 keV range exceeds that predicted by PC models by a few orders of magnitude (see discussion in Zavlin & Pavlov 1997, hereafter ZP97), proved its X-rays to be of a magnetospheric origin. Thus, thorough investigations are needed in each specific case to ascertain the nature of the observed radiation.

The closest known millisecond pulsar, J0437–4715 ($P = 5.75$ ms, $\tau = P/2\dot{P} = 5 \times 10^9$ yr, $\dot{E} = 4 \times 10^{33}$ ergs s $^{-1}$, $B \sim 3 \times 10^8$ G, $d = 180$ pc), is of special interest. Important

data from this pulsar have been collected with the *ROSAT* (Becker & Trümper 1993; Becker et al. 1997), *EUVE* (Edelstein, Foster, & Bowyer 1995; Halpern, Martin, & Marshall 1996) and *ASCA* (Kawai, Tamura, & Saito 1997) space observatories. Becker & Trümper (1993) and Halpern et al. (1996) showed that the spectral data can be fitted with power-law or blackbody plus power-law models. The latter fit indicates that the X-ray emission may be, at least partly, of a thermal (PC) origin. Rajagopal & Romani (1996) applied more realistic models of radiation emitted by NS atmospheres to fitting the thermal component and concluded that the iron atmospheres do not fit the observed spectrum.

The observations made with the *ROSAT* and *EUVE* missions revealed smooth pulsations of soft X-rays with the pulsed fraction $f_p \sim 25\%$ – 50% apparently growing with photon energy in the 0.1–2.4 keV *ROSAT* range. Since the pulsed fraction of the nonthermal radiation is not expected to vary significantly in the narrow energy range, it is natural to attribute the observed radiation to the pulsar PCs. The PC radiation should inevitably be pulsed unless the rotation axis coincides with either the line of sight or magnetic axis. If it were the blackbody (isotropic) radiation, the pulsed fraction would remain the same at all photon energies. The energy dependence of f_p can be caused by anisotropy (limb darkening) of thermal radiation emitted from NS atmospheres (Pavlov et al. 1994; Zavlin, Pavlov, & Shibano 1996). Zavlin et al. (1996) showed that even in the case of low magnetic fields characteristic of millisecond pulsars ($B \sim 10^8$ – 10^9 G), the anisotropy strongly depends on photon energy and chemical composition of NS surface layers. To interpret the *ROSAT* and *EUVE* observations of PSR J0437–4715, ZP97 applied the NS atmosphere models, accounting for the energy-dependent limb darkening and the effects of gravitational redshift and bending of photon trajectories (Zavlin, Shibano, & Pavlov 1995). Assuming a viewing angle (between the rotation axis and line of sight) of $\zeta = 40^\circ$ and magnetic inclination (angle between the magnetic and rotation axes) of $\alpha = 35^\circ$, inferred by Manchester & Johnston (1995) from the phase dependence of the position angle of the radio polarization, ZP97 showed that both the spectra and the light curves (pulse profiles) of the *entire* soft X-ray radiation detected by *ROSAT* and *EUVE* can be interpreted as thermal radiation

from two hydrogen-covered PCs, whereas neither the black-body nor iron atmosphere models fit the observations. The approach of ZP97 differs substantially from that of Rajagopal & Romani (1996), who did not take into account the energy-dependent anisotropy of the emergent radiation and gravitational bending (hence, they could not analyze the pulse profiles), made the unrealistic assumption that pulsed and unpulsed flux components are of completely separate origin and consequently obtained quite different parameters of the radiating region. The simplest, single-temperature PC model of ZP97 provides a satisfactory fit with the typical PC radius of $R_{\text{pc}} \sim 1$ km (reasonably close to the theoretical estimate of 1.9 km) and temperature of $T_{\text{pc}} \sim 1 \times 10^6$ K. The corresponding bolometric luminosity of the two PCs, $L_{\text{bol}} = (1.0\text{--}1.6) \times 10^{30}$ ergs s^{-1} , comprises $\sim (2\text{--}4) \times 10^{-4}$ of the pulsar total energy loss, \dot{E} . This value of L_{bol} is in excellent agreement with the predictions of the slot-gap pulsar model by Arons (1981). Even better fit to the observational data is provided by a model with nonuniform temperature distribution along the PC surface. In addition, the inferred interstellar hydrogen column density toward the PSR J0437–4715, $n_{\text{H}} \sim (1\text{--}3) \times 10^{19} \text{ cm}^{-2}$, was demonstrated to be consistent with the properties of the interstellar medium obtained from observations of other stars in the vicinity of the pulsar. All these results allow one to conclude that the X-ray radiation observed from PSR J0437–4715 is indeed of the thermal (PC) origin.

The results of ZP97 were obtained for fixed orientations of the rotation and magnetic axes (angles ζ and α) and for standard NS mass of $M = 1.4 M_{\odot}$ and radius of $R = 10$ km. The inferred PC radius, temperature, and luminosity are almost insensitive to these four parameters. Their main effect is on the shape and pulsed fraction of the light curves. For instance, f_p decreases with increasing the mass-to-radius ratio, unless the observer can see the PC in the center of the back hemisphere of the NS, which is possible at $\alpha \approx \zeta$ and $M_*/R_{10} > 1.93$, where $M_* = M/M_{\odot}$ and $R_{10} = R/(10 \text{ km})$ (see, e.g., Zavlin et al. 1995). The angles α and ζ cannot be precisely evaluated from the radio polarization measurements because of the complicated variation of the polarization position angle across the eight-component mean radio pulse of PSR J0437–4715 (Manchester & Johnston 1995), and the true NS mass and radius may differ from the canonical values. On the other hand, the fact that the set of angles and M/R adopted by ZP97 fit the data does not mean that a better fit cannot be obtained for another set, and it tells us nothing about the allowed domain of these parameters. Hence, fitting the light curves for variable M/R , α , and ζ enables one to constrain the mass-to-radius ratio and/or the magnetic inclination and viewing angle, so that the present Letter is complementary to ZP97. We describe our approach in § 2 and present the results on PSR J0437–4715 in § 3.

2. METHOD

Since the shape of the light curves depends on energy, the light curve fitting is coupled to the spectral fitting. We fit the count rate spectrum (total of ≈ 3200 counts) collected by the *ROSAT* Position Sensitive Proportional Counter (PSPC) with the phase-integrated model spectrum emitted from two identical, uniformly heated PCs 180° apart, assuming the hydrogen composition of the surface layers (ZP97). The fitting is carried out on a grid of angles ζ and α between 0° and 90° at different mass-to-radius ratios M_*/R_{10} in a range allowed by equations of state of the superdense NS matter. As shown in ZP97, both the *ROSAT* and *EUVE* observations of PSR J0437–4715 are

consistent with the applied model at the interstellar hydrogen column density of $\sim 1 \times 10^{19} \text{ cm}^{-2}$; therefore we freeze n_{H} at this value and obtain T_{pc} and R_{pc} from the spectral fits for each set of ζ , α , and M_*/R_{10} . With these T_{pc} and R_{pc} , we calculate the model spectral fluxes for various phases of the pulsar period and fold each of the spectra with the PSPC response matrix; this gives us the model light curve as a function of phase ϕ for given ζ , α , and M_*/R_{10} . This light curve is then compared with the observed PSPC light curve. For this comparison, we used the PSPC light curve for the total *ROSAT* energy range, 0.1–2.4 keV; its pulsed fraction (for 17 phase bins) was determined to be $f_p = 30\% \pm 4\%$ (ZP97). We bin the model light curve to the same number of phase bins ($K = 17$) and calculate the χ^2 value,

$$\chi^2 = \sum_{k=1}^K \frac{(N_{k,o} - N_{k,m})^2}{N_{k,o}}, \quad (1)$$

for each set of ζ , α , and M_*/R_{10} ($N_{k,o}$ and $N_{k,m}$ are the observed and model numbers of counts in the k th bin). This allows us to find the best-fit parameters (which correspond to the minimum of χ^2) and confidence levels in the parameter space.

3. RESULTS

Figure 1 shows the 68%, 90%, and 99% confidence regions for the above-described light curve models in the ζ - α plane at several values of the mass-to-radius ratio, $M_*/R_{10} = 1.1, 1, 2, \dots, 1.6$. The ratio determines the parameter $g_r = (1 - 0.295 M_*/R_{10})^{1/2}$ responsible for the effects of gravitational redshift and bending of photon trajectories (e.g., Zavlin et al. 1995). For the M_*/R_{10} values in Figure 1, the parameter g_r varies between 0.82 and 0.73, making visible from 74% to 91% of the whole NS surface, so that a distant observer can detect the radiation from both PCs simultaneously during almost the whole pulsar period. The plots in Figure 1 are clearly symmetrical with respect to the transformation $\zeta \leftrightarrow \alpha$ because the model light curves depend only on the angle θ between the observer's direction and the magnetic axis: $\cos \theta = \cos \zeta \cos \alpha + \sin \zeta \sin \alpha \cos \phi$, where ϕ is the rotational phase. The minimum value of the reduced χ^2 ($\chi_r^2 = 1.07$ for 17 degrees of freedom) was obtained at $\zeta = 47^\circ$, $\alpha = 18^\circ$ (or vice versa), and $M_*/R_{10} = 1.2$ ($g_r = 0.80$). In Figure 1 we also show the lines of constant model pulsed fraction. The lines for the pulsed fractions compatible with the detected value, $f_p = 30\% \pm 4\%$, are close to the confidence contours unless ζ and/or α are close to 90° ; at these large angles the model light curves have a complicated shape (e.g., two maxima per rotational period) inconsistent with what is observed. The increase of the mass-to-radius ratio enhances the gravitational bending and leads to a greater contribution from the secondary PC (that on the back NS hemisphere), which suppresses the model pulsations. As a result, the allowed regions in Figure 1 completely vanish at $M_*/R_{10} > 1.6$ ($g_r < 0.73$).¹ With decreasing the M_*/R_{10} ratio, the confidence regions shift toward the bottom left-hand corner of the ζ - α plane reaching a limiting position at $M_*/R_{10} \approx 0.3$ ($g_r \approx 0.95$) when the effect of the gravitational bending becomes negligible, and the observer detects radiation only from the primary PC (on the front hemisphere).

Figure 1 provides obvious constraints on the pulsar mass-

¹ In fact, at $M_*/R_{10} \gtrsim 1.93$ ($g_r \lesssim 0.66$) the model pulsations may grow because of the appearance of strong narrow peaks from PC at $\theta \approx 180^\circ$. However, there are no such peaks in the observed light curve.

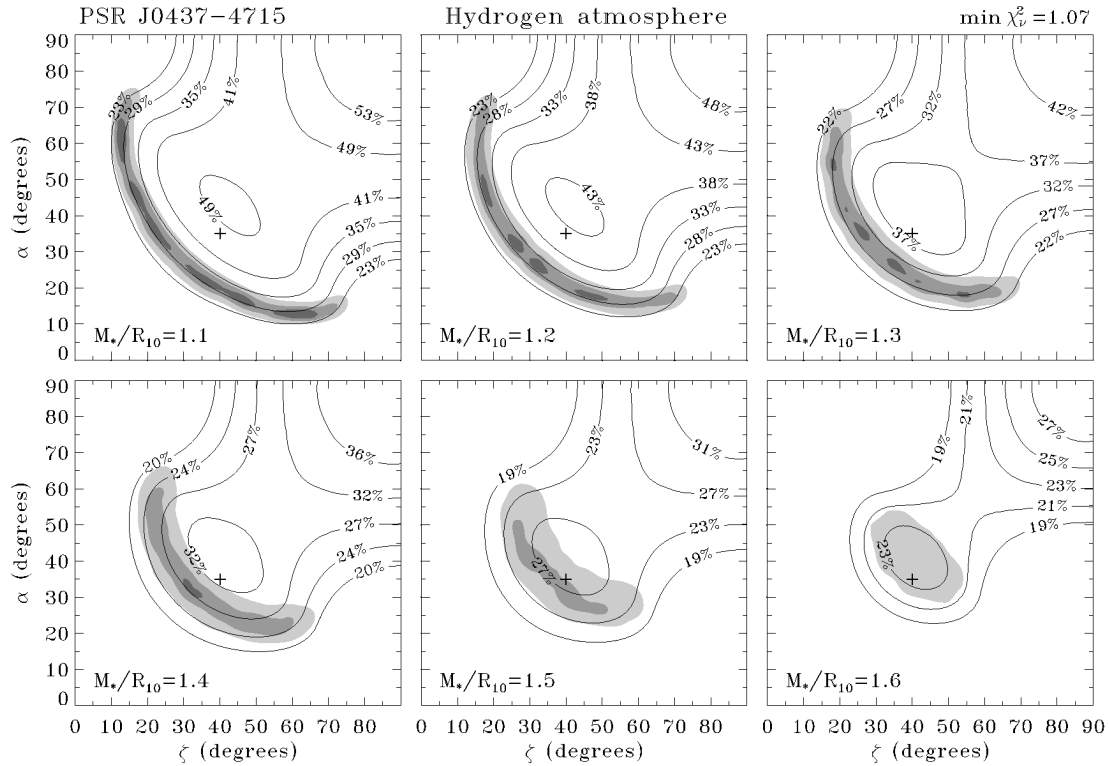


FIG. 1.—68%, 90%, and 99% confidence regions (dark, medium, and light gray, respectively) in the ζ - α plane for different values of the M_*/R_{10} ratio. The lines with numbers show the values of constant pulsed fractions. The crosses mark the points with $\zeta = 40^\circ$ and $\alpha = 35^\circ$.

to-radius ratio. For instance, if there were no observational information about the ζ and α values, the only constraint would be $M < 1.6 M_\odot$ ($R/10 \text{ km}$), or $R > 8.8(M/1.4 M_\odot) \text{ km}$, at a 99% confidence level. If, however, we adopt $\zeta = 40^\circ$ and

$\alpha = 35^\circ$, as given by Manchester & Johnston (1995), then $1.4 < M_*/R_{10} < 1.6$. Figure 2 shows the corresponding domain in the NS mass-radius diagram, restricted by the $M(R)$ dependences for soft (π) and hard (MF) equations of state of the superdense matter (Shapiro & Teukolsky 1983). It follows from this picture, for example, that the radius of an NS with the canonical mass of $M = 1.4 M_\odot$ is within the range $8.8 < R < 10.0 \text{ km}$.

Another set of angles, $\zeta = 24^\circ$ and $\alpha = 20^\circ$, was suggested by Gil & Krawczyk (1997). This set gets within the 99% confidence region only for very low mass-to-radius ratios, $M_*/R_{10} < 0.3$, when the gravitational effects become negligible. This corresponds to very low masses, $M < 0.5 M_\odot$ at any R allowed by the equations of state (Fig. 2).

Note that for these angles and $M_*/R_{10} < 1.8$, the secondary PC remains invisible during the whole pulsar period.

4. CONCLUSIONS

We have demonstrated that the analysis of the soft X-ray radiation emitted by PCs of radio pulsars in terms of NS atmosphere models provides a new tool to constrain the NS mass and radius and, consequently, the equation state of the superdense matter in the NS interiors. The constraints become more stringent if this analysis is combined with complementary data on the pulsar magnetic inclination and viewing angle, as we have shown using the millisecond pulsar J0437–4715 as an example. In principle, these angles can be inferred from the phase dependence of the radio polarization position angle. However, in the case of J0437–4715, this dependence is too complicated to be described by a simple rotating vector model of Radhakrishnan & Cooke (1969), so the inferred angles are very uncertain. Once an adequate model for the radio emission

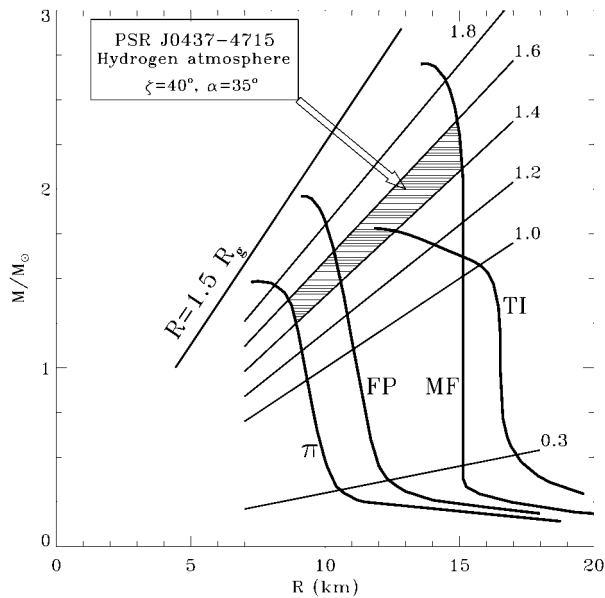


FIG. 2.—NS mass-radius diagram with straight lines of constant M_*/R_{10} ratio (numbers near the lines) and $M(R)$ curves for a few equations of state of superdense matter: soft (π), intermediate (FP), and hard (TI and MF). The line $R = 1.5 R_g$ (R_g is the gravitational radius) shows the most conservative lower limit on the NS radius at a given mass. The hatched region shows the mass-radius domain for PSR J0437–4715 allowed by the light curve fitting at $\zeta = 40^\circ$ and $\alpha = 35^\circ$.

is found, the statistical analysis of the polarization data would result in a domain of allowed angles in the ζ - α plane, and the constraints should be based on overlapping of the confidence regions obtained from the X-ray light curve and from the radio polarization data. This may constrain not only the M/R ratio but also the pulsar geometry.

The allowed $M(R)$ domain can be further restricted if additional information on the NS mass is available. For instance, since PSR J0437–4715 is in a binary system with a white dwarf companion, it is possible to estimate independently an upper limit on the NS mass. Sandhu et al. (1997) found upper limits on the white dwarf mass, $M_{\text{wd}} \leq 0.32 M_{\odot}$, and on the orbital inclination, $i \leq 43^{\circ}$, that yields a restriction $M < 2.5 M_{\odot}$ (see their Fig. 2). If further observations of the pulsar reduce the limit on i , or a lower upper limit on M_{wd} is obtained from white dwarf cooling models, a more stringent constraint on M would follow, thus narrowing the allowed domains of the other pulsar parameters (R , ζ , and α).

The above-described analysis for PSR J0437–4715 is simplified by the pulsar's low magnetic field, which does not affect the properties of the X-ray radiation. The spectra and, in particular, angular distribution of radiation emerging from strongly magnetized NS atmospheres depends significantly on the magnetic field (Pavlov et al. 1994). Thus, a similar, albeit more complicated, analysis of X-ray radiation from pulsars with strong magnetic fields, $B \sim 10^{11}$ – 10^{13} G (e.g., PSR B1929+10 and 0950+08), would enable one to constrain also the magnetic field strength at their magnetic poles.

We thank Werner Becker for providing us with the *ROSAT* PSPC light curve. We are grateful to Joachim Trümper for stimulating discussions. The work was partially supported through NASA grant NAG5-2807, INTAS grant 94-3834, and DFG-RBRF grant 96-02-00177G. V. E. Z. acknowledges a Max-Planck fellowship.

REFERENCES

- Arons, J. 1981, *ApJ*, 248, 1099
 Becker, W., & Trümper, J. 1993, *Nature*, 365, 528
 ———. 1997, *A&A*, 326, 682
 Becker, W., et al. 1997, in preparation
 Beskin, V. S., Gurevich, A. F., & Istomin, Ya. N. 1993, *Physics of Pulsar Magnetosphere* (Cambridge: Cambridge Univ. Press)
 Cheng, A. F., & Ruderman, M. A. 1980, *ApJ*, 235, 576
 Edelstein, J., Foster, R. S., & Bowyer, S. 1995, *ApJ*, 454, 442
 Gil, J., & Krawczyk, A. 1997, *MNRAS*, 285, 561
 Greiveldinger, C., et al. 1996, *ApJ*, 465, L35
 Halpern, J. P., Martin, C., & Marshall, H. L. 1996, *ApJ*, 462, 908
 Kawai, N., Tamura, K., & Saito, Y. 1997, in *ESA-SP 1194*, ESA's Report to the 31st COSPAR Meeting, ed. W. R. Burke (Noordwijk: ESA), in press
 Manchester, R. N., & Johnston, S. 1995, *ApJ*, 441, L65
 Manning, R. A., & Willmore, A. P. 1994, *MNRAS*, 266, 635
 Michel, F. C. 1991, *Theory of Neutron Star Magnetospheres* (Chicago: Univ. Chicago Press)
 Pavlov, G. G., Shibano, Yu. A., Ventura, J., & Zavlin, V. E. 1994, *A&A*, 289, 837
 Radhakrishnan, V., & Cooke, D. J. 1969, *Astrophys. Lett.*, 3, 225
 Rajagopal, M., & Romani, R. W. 1996, *ApJ*, 461, 327
 Saito, Y., et al. 1997, *ApJ*, 477, L37
 Sandhu, J. S., et al. 1997, *ApJ*, 478, L95
 Shapiro, S., & Teukolsky, S. 1983, *Black Holes, White Dwarfs and Neutron Stars* (New York: Wiley)
 Wang, F. Y.-H., & Halpern, J. P. 1997, *ApJ*, 482, L159
 Yancopoulos, S., Hamilton, T. T., & Helfand, D. 1994, *ApJ*, 429, 832
 Zavlin, V. E., & Pavlov, G. G. 1997, *A&A*, in press (ZP97)
 Zavlin, V. E., Pavlov, G. G., & Shibano, Yu. A. 1996, *A&A*, 315, 141
 Zavlin, V. E., Shibano, Yu. A., & Pavlov, G. G. 1995, *Astron. Lett.*, 21, 149